

A study of the inhibition of copper corrosion by triethyl phosphate and triphenyl phosphate self-assembled monolayers

WENJUAN GUO¹, SHENHAO CHEN^{1,2,*} and HOUYI MA¹

¹Department of Chemistry, Shandong University, Jinan, Shandong, 250100, P. R. China and

²State Key Laboratory for Corrosion and Protection of Metals, Shenyang, 110015, P. R. China
(E-mail: shchen@sdu.edu.cn)

(Received 28 January, revised 20 May 2005)

Abstract: Two kinds of phosphates, triethyl phosphate (TEP) and triphenyl phosphate (TPP), were used to form self-assembled monolayers for the inhibition of the corrosion of copper in 0.2 mol dm⁻³ NaCl solution. Electrochemical impedance spectroscopy (EIS) was applied to investigate the inhibition effects. The results showed that their inhibition ability first increased with increasing immersion time in ethanolic solutions of the corresponding compounds. However, when the immersion time was increased over some critical point, the inhibition effect decreased. For the same immersion time, the inhibition effect of the TPP monolayer was more pronounced than that of the TEP monolayer. Thus, *ab initio* calculations were used to interpret the relationship between the inhibition effects and the structures of the compounds.

Keywords: copper, phosphates, self-assembled monolayers (SAMs), electrochemical impedance spectroscopy (EIS), *ab initio* calculation.

INTRODUCTION

The problem of metal corrosion is a significant research topic. Copper is widely used in the chemical and electronic industry due to its high thermal and electrical conductivity and low cost. However, copper is an active metal which tends to be corroded and oxygenated easily when exposed to air or water.^{1–3} Some kinds of compounds can spontaneously adsorb on the metal surface and form the self-assembled monolayers (SAMs). SAMs are the molecule-scale barrier against corrosion and oxidation. Most of the compounds forming SAMs contain nitrogen, sulfur or oxygen.⁴ A lot of research has been done with *n*-alkanethiol SAMs.^{1,5–11} In our group, the investigations involved carbazole, *N*-vinylcarbazole, several kinds of Schiff bases and surfactants.^{12–15} Considering the extensive applications of aqueous environments, Lusk and Jennings¹⁶ investigated the SAMs formed by a series of sodium S-alkyl thiosulfates, which are water-soluble inhibitors. This provided a

* Corresponding author: Fax: +86-531-8565167. Tel. +86-531-8364959.

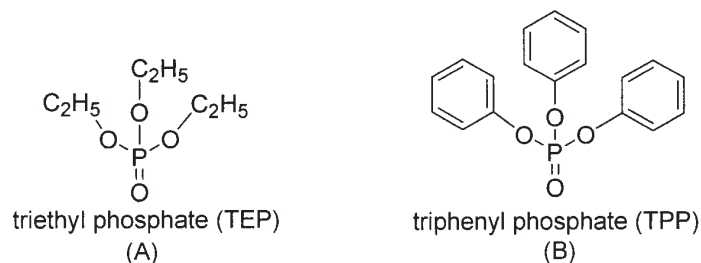


Fig. 1. Molecular structures of (A) TEP and (B) TPP.

new field of choice of inhibitors. To sum up, the SAM technique has remarkable advantages. Thus, it has become the focus of many interrelated research fields.

In this study, it was found that two kinds of phosphates, triethyl phosphate (TEP) and triphenyl phosphate (TPP), inhibited copper corrosion in chloride solution. They are the homologous series of compounds and their structural formulas are shown in Fig. 1. The advantage of these compounds compared with traditional inhibitors is that they do not release strong, unpleasant odors and their toxicity is correspondingly low. The purpose of this research was to exploit a series of new compounds suitable for forming SAMs which have lower toxicity and a higher efficiency for the inhibition of copper corrosion. The inhibition effects of these films were compared by using electrochemical impedance spectroscopy (EIS). Simultaneously, *ab initio* calculations were applied to examine the self-assembling mechanism at the theoretical level and to explained the relationship between the inhibition effects and the molecular structure.

EXPERIMENTAL

Chemicals

All the chemicals were used as received. The compounds, TEP and TPP, were dissolved in the absolute ethanol (A.R.) to form 1×10^{-3} mol dm⁻³ ethanolic solutions. A sodium chloride solution, 0.2 mol dm⁻³, and a nitric acid solution, 7 mol dm⁻³, were prepared with tridistilled water.

Preparation of the electrodes

A copper rod of 5 mm diameter was embedded in epoxy resin, leaving only its cross-section to serve as the working electrode. Prior to every experiment, the exposed surface was polished with silicon carbide waterproof abrasive papers, grid 800 to 2000.

Formation of the self-assembled monolayers

The preparation of SAMs was carried out in the following way. The copper electrode was first polished until its surface became smooth and mirror-like bright, rinsed with tridistilled water and then etched in a 7 mol dm⁻³ HNO₃ solution for about 20 s to obtain a fresh and oxide-free copper surface.³⁵ It was then rinsed with tridistilled water and absolute ethanol as quickly possible and immediately immersed in an ethanolic solution containing the required compound to form SAMs. The ethanolic solutions were deoxygenated by purging with nitrogen. After the designated time, the SAMs-covered electrode was taken out and rinsed with absolute ethanol and tridistilled water to remove physically adsorbed molecules from the surface. Then it was dried in a steam of nitrogen. Finally the electrode was placed into an electrochemical cell for performing the electrochemical measurements at room temperature (25 ± 1 °C).

EIS measurements

The cell for electrochemical measurements was a traditional three-electrode glass cell. A naked copper electrode or a copper electrode covered with SAMs was used as the working electrode; the counter electrode was a platinum plate and the reference electrode was a saturated calomel electrode (SCE). The reference electrode was led to the surface of the working electrode through a Luggin capillary. The potentials reported in this paper are all referred to the SCE. The whole measurement process was in a still electrolyte system at room temperature (25 ± 1 °C). The electrolyte, NaCl solution, was opened to the air during each experiment.

EIS measurements were performed with an IM6 electrochemical measurement system (ZAHNER, Germany electrochemical workstation). Before each measurement, the copper electrode either without or with SAMs, was immersed in 0.2 mol dm^{-3} NaCl solution and equilibrated for 30 min. After this time, the open-circuit potentials were almost invariable. This step provides a steady system for the whole experiment. The sinusoidal potential perturbation was 5 mV in amplitude around the corresponding open-circuit potential and the frequency ranged from 60 kHz to 20 mHz. The impedance data were fitted in accordance with the corresponding equivalent circuits using fitting software.

RESULTS AND DISCUSSION

EIS results

EIS is an electrochemical measurement technique which can directly measure the solution resistance (R_s), the charge-transfer resistance (R_{ct}), and the double-layer capacitance (C_{dl}). From R_{ct} and the corresponding formula, the film coverage (θ) on the electrode can be calculated. θ reflects the assembly effect of the film. C_{dl} can also be used to determine the quality of a film.^{1,8,17,18}

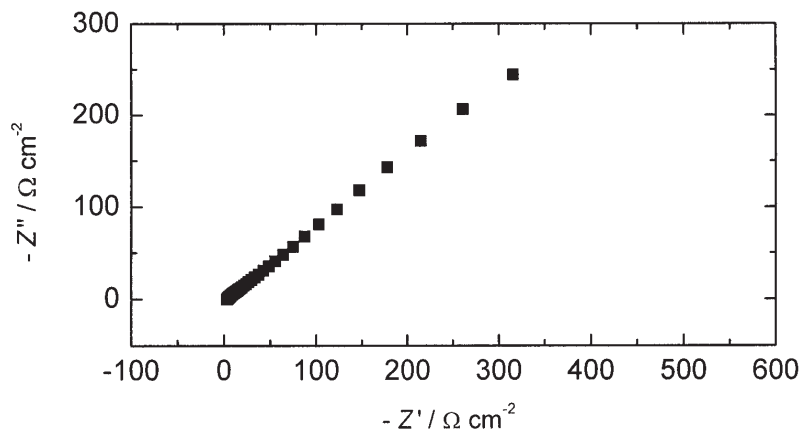


Fig. 2. Nyquist impedance spectrum of the naked copper electrodes in 0.2 mol dm^{-3} NaCl solution.

As is shown in Fig. 2, the Nyquist impedance plot for naked copper appears in the form of a straight-line, since the high frequency capacitive loop is poorly defined due to a fast electrode reaction.²⁴ The small semicircle in the high frequency region is attributed to the time constant, ($R_{ct} C_{dl}$), which is related to both R_{ct} and C_{dl} .^{17,18} The value of R_{ct} is approximately equal to the diameter of the small semicircle. The straight-line appearing in the low frequency region is called “Warburg imped-

ance". Bertocci *et al.*²³ considered that copper corrosion in oxygenated chloride solutions occurred at rates lower than the mass transfer limited oxygen diffusion rate and that the reduction of oxygen to peroxide was the dominant cathodic process. This means that the diffusion impedance in the Nyquist plots reflects the mass transfer limited diffusion rate of CuCl_2^- complexed species, while the anodic diffusion process mainly involves the diffusion of soluble copper species (CuCl_2^-) from the surface of the electrode to the bulk solution.^{19–22} This plot can be analyzed with the equivalent circuit shown in Fig. 5 (A),²⁵ where R_{ct} stands for the charge-transfer resistance, CPE_{dl} is a constant phase element, W the Warburg impedance and R_s is the solution resistance. Here, CPE_{dl} is substituted for C_{dl} to give a more accurate fit.²⁶ In most cases, the capacitive loops are depressed semicircles rather than regular semicircles, which is related to a phenomenon called the "dispersion effect". The admittance of CPE_{dl} is described as:

$$Y_Q = Y_0 (j \omega)^n \quad (1)$$

where j is the imaginary root, ω the angular frequency, Y_0 the magnitude and n the exponential term.²⁷ The value of n is related to the surface roughness of the electrode²⁷ and it ranges from 0 to 1. The higher the value of n , the smoother is the electrode surface. However, SAMs were found to contain molecule-sized defects^{28–30} and in reality it is impossible for the value of n to be 1.

A series of Nyquist impedance plots of copper electrodes with SAMs of TEP and TPP in 0.2 mol dm^{-3} NaCl solution are shown in Figures 3 and 4, respectively. When the electrode surface was covered with a film, the value of R_{ct} increases rapidly. In Fig. 3(C), the plot displays only one capacitive loop and it can be analyzed with the simple equivalent circuit in Fig. 5(B). In fact, SAMs formed at the electrode surface can act as a barrier layer between the electrode and the solution and efficiently hinder the attack of the substrate by chloride ions. The disappearance of the Warburg impedance may imply the formation of better films coated on the electrodes.

All the EIS data can be fitted according to the related equivalent circuits in Fig. 5. The results were listed in Table I. θ can be calculated from the following formula:³¹

$$(1 - \theta) = R_{\text{ct}}^0 / R_{\text{ct}} \quad (2)$$

where R_{ct}^0 is the charge-transfer resistance of the naked electrode and R_{ct} is the charge-transfer resistance of a copper electrode covered with SAMs. The increase of θ can reflect the increase of the number of the molecules adsorbed on Cu and the improvement of the inhibition effect.

As can be seen from Table I, the charge-transfer impedance of the naked electrode has the lowest value, while that of SAMs-covered copper are higher to some extent. With increasing immersion time, the value of R_{ct} increased. On increasing the immersion time from 1 h to 12 h, the value of θ of the TEP-covered and TPP-covered copper electrodes increased from 81.0 % to 93.8 % and from 85.4 to

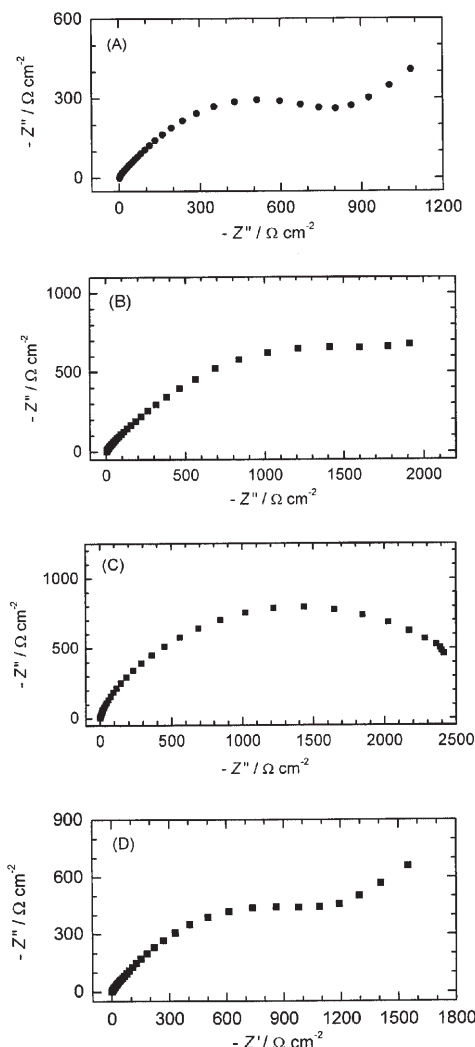


Fig. 3. Nyquist impedance spectra of TEP-covered copper electrodes in 0.2 mol dm^{-3} NaCl solution. The copper electrode was immersed in the ethanolic TEP solution for different times: (A) 1 h; (B) 4 h; (C) 12 h; (D) 24 h.

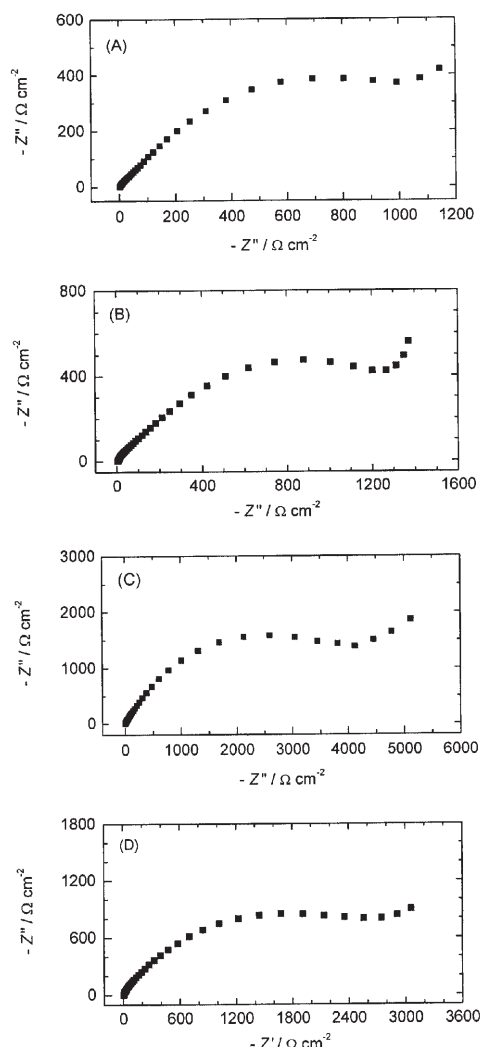


Fig. 4. Nyquist impedance spectra of TPP-covered copper electrodes in 0.2 mol dm^{-3} NaCl solution. The copper electrode was immersed in the ethanolic TPP solution for different times: (A) 1 h; (B) 4 h; (C) 12 h; (D) 24 h.

96.5 %, respectively. This implies that the films formed on the electrodes became denser. This phenomenon can be understood as following: the longer the immersion time, the more molecules cover the copper surface and the inhibition effect is better. However, when the immersion time was increased to 24 h, θ decreased instead of increasing, which is caused by the "steric effect". Namely, if the number of the adsorbed molecules increases beyond a certain value, the tail groups crowd

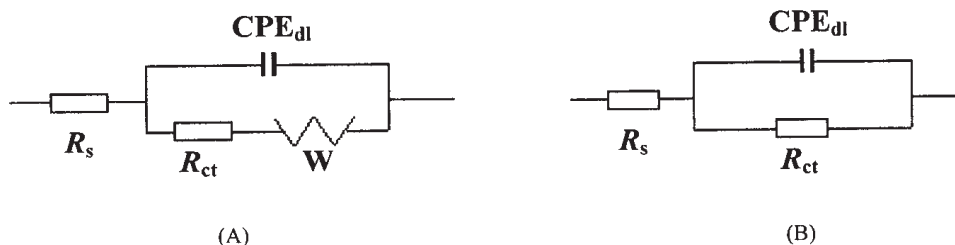


Fig. 5. (A) The equivalent circuit to fit the EIS for copper displaying a Warburg impedance; (B) The simple equivalent circuit to fit the EIS for copper displaying one capacitive loop.

each other which may cause a rearrangement of the TEP and TPP molecules. As a result, it is easier for corrosive chloride ions to attack the copper substrate through the interspaces between the tail groups of the adsorbed molecules. Comparing the values of θ for TEP with those for TPP, it was found that, for the same immersion time in the compound-containing solutions the value of θ for TPP was generally larger than those for TEP. Judging from the structures of the two molecules in Fig. 1, the tail groups of TPP molecule are much larger than those of the TEP molecule. When the TPP molecules adsorbed onto a metal surface, the larger tail groups can coat a wider area of the metal surface. Thus the inhibition effect is related to the special structure of the adsorbed molecules.

TABLE I. The fitting results of the impedance spectra shown in Figs. 2–4 in accordance with the related equivalent circuit shown in Fig. 5

Compounds	Immersion time/h	$R_s/\Omega \text{ cm}^2$	$R_{ct}/\Omega \text{ cm}^2$	CPE_{dl}		$\theta/\%$
				$Y_0/10^{-6} \Omega^{-1} \text{ cm}^{-2} \text{ s}^n$	$n (0-1)$	
Naked	0	2.89	138	3790	0.49	0
TEP	1	1.26	728	277	0.69	81.0
	4	3.67	1412	330	0.65	90.2
	12	1.44	2218	52.9	0.81	93.8
	24	1.08	936	231	0.71	85.3
	24	1.08	936	231	0.71	85.3
TPP	1	1.21	943	502	0.64	85.4
	4	4.47	1159	215	0.66	88.1
	12	3.99	3958	75.5	0.74	96.5
	24	4.11	2011	85.7	0.72	93.1

Quantum chemical calculations

In order to examine the self-assembling mechanism of TEP and TPP molecules on a copper surface, *ab initio* calculations were performed. By using the density functional theory method combined with all electron bases under the local density approximation, the Mulliken charge distributions on the TEP and TPP molecules were obtained (see Fig. 6).

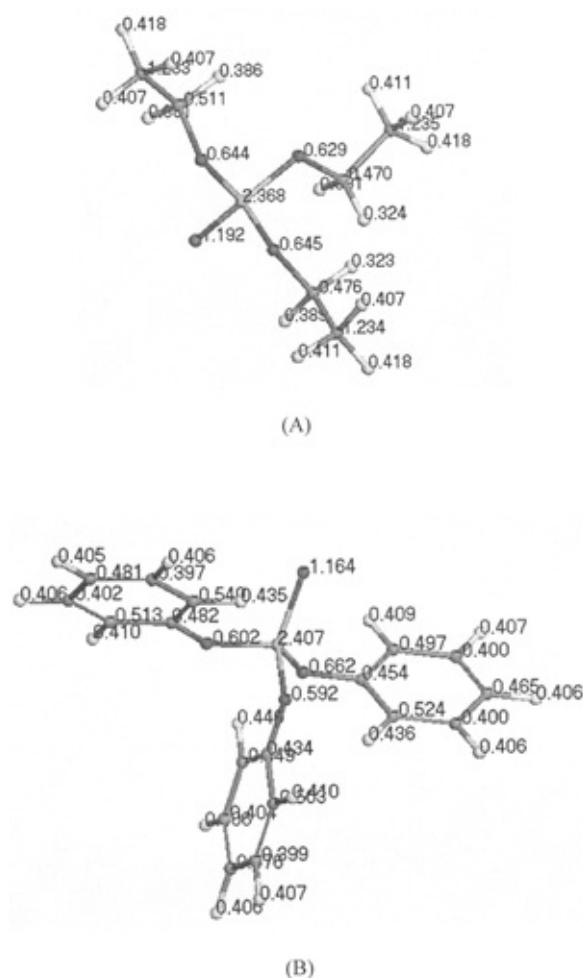


Fig. 6. The total atomic charges of (A) TEP and (B) TPP, obtained by *ab initio* calculations.

It is well-known that the more negative the atomic partial charges of the adsorbed centre are, the easier is the donation of electrons from the atom to the unoccupied orbital of the surface atoms of the metal. The atomic partial charges of the TEP molecule are shown in Fig. 6. The oxygen atom at the end of the TEP molecule has a partial charge of -1.192 e and the atomic partial charges of the three carbon atoms in the three $-\text{CH}_3$ groups are -1.233 e, -1.234 e and -1.235 e. Although the atomic partial charges on the carbon atoms are more negative than that of the oxygen atom at the end of the TEP molecule, there are three hydrogen atoms bonded to each carbon atom, which makes the reaction of the carbon atoms with the copper surface more difficult. Concerning the TPP molecule, the atomic partial charge of the oxygen atom at the end of the TPP molecule is -1.164 e, which is much more negative than any other atom of the molecule. Hence, it is suggested that both the TEP and TPP molecule react with the copper surface *via* the oxygen atom at the end of the molecule.

Furthermore, according to the Fukui frontier orbital approximation,³² the most active and the first reactive molecular orbitals are the highest occupied molecular orbital (HOMO) and the lowest unoccupied molecular orbital (LUMO), which are generally called the frontier Molecular Orbitals (MO). It is known that a metal can accept electrons from the HOMO of an electron donor into its LUMO and, simultaneously, the metal can donate its electrons to the LUMO of the compound. The former condition plays the dominant role during the reaction. Vosta^{33,34} pointed out that the higher the HOMO energy of the compound molecule, the stronger is the bonding between the compound and the surface atoms of a metal. By the quantum chemical calculations, it was found that the HOMO energies of the TEP and TPP molecule are -10.516 eV and -10.010 eV and their LUMO energies are -3.744 eV and -5.904 eV, respectively. This results indicates that TPP molecules adsorb onto a copper electrode more easily than TEP molecules do. This conclusion is in accordance with the experimental results.

CONCLUSION

With increasing immersion time of Cu in a TEP-containing or a TPP-containing ethanolic solution, more molecules assembled on the copper surface and the value of θ became larger and the inhibition effect initially became better. The highest inhibition efficiencies of TEP and TPP SAMs in 0.2 mol dm^{-3} NaCl solution were 93.8 % and 96.5 %, respectively. However, there was a critical value of the immersion time beyond which the value of θ decreased. The different tail groups of the compounds can result in a change in the barrier properties. The inhibition effect of TPP is better than that of TEP under the same assembling conditions. The *ab initio* calculations provided a theoretical explanation for the inhibition effect of TEP and TPP SAMs.

Acknowledgements: This work was supported by the Chinese National Natural Science Fund (No. 20373038).

ИЗВОД

ПРОУЧАВАЊЕ ИНХИБИЦИЈЕ КОРОЗИЈЕ БАКРА САМОУРЕЂЕНИМ МОНОСЛОЈЕВИМА ТРИЕТИЛ-ФОСФАТА И ТРИФЕНИЛ-ФОСФАТА

WENJUAN GUO¹, SHENHAO CHEN^{1,2} и HOUYI MA¹

¹Department of Chemistry, Shandong University, Jinan, Shandong, 250100, P. R. China and ²State Key Laboratory for Corrosion and Protection of Metals, Shenyang, 110015, P. R. China

Самоуређени монослојеви два фосфатна једињења, триетил-фосфата (ТЕП) и трифенил-фосфата (ТПП), су коришћени као инхибитори корозије бакра у раствору $0,2 \text{ mol dm}^{-3}$ NaCl. Ефекат инхибиције је испитиван методом спектроскопије електрохемијске импеданције (SEI). Резултати су показали да са повећањем времена урањања електроде у раствор поменутих једињења у етанолу расте степен инхибиције, али само до неког критичног времена, након којег степен инхибиције почиње да опада. При истом времену формирања монослоја, TPP је показао већи инхибициони ефекат него ТЕР. Веза између инхибиционог ефекта и структуре једињења је објашњен *ab initio* прорачуном.

(Примљено 28. јануара, ревидирано 20. маја 2005)

REFERENCES

1. P. E. Laibinis, G. M. Whitesides, *J. Am. Chem. Soc.* **114** (1992) 9022
2. Y.-T. Tao, *J. Am. Chem. Soc.* **115** (1993) 4350
3. P. E. Laibinis, G. M. Whitesides, D. L. Allara, Y.-T. Tao, A. N. Parikh, R. G. Nuzzo, *J. Am. Chem. Soc.* **113** (1991) 7152
4. M. Lagrnee, B. Mernari, M. Bouanis, M. Traisnel, F. Bentiss, *Corros. Sci.* **44** (2002) 573
5. G. K. Jennings, P. E. Laibinis, *Colloids Surf. A* **116** (1996) 105
6. J. Scherer, M. R. Vogt, O. M. Magnussen, R. J. Behm., *Langmuir* **13** (1997) 7045
7. Y. Q. Feng, W. K. Teo, K. S. Siow, Z. Q. Gao, K. L. Tan, A. K. Hsieh, *J. Electrochem. Soc.* **114** (1997) 55
8. Y. Yamamoto, H. Nishihara, K. J. Aramaki, *J. Electrochem. Soc.* **140** (1993) 436
9. M. Itoh, H. Nishihara, K. Aramaki, *J. Electrochem. Soc.* **141** (1994) 2018
10. H. Y. M, C. Yang, B. S. Yin, G. Y. Li, S. H. Chen, J. L. Luo, *Appl. Surf. Sci.* **218** (2003) 143
11. G. K. Jennings, J. C. Munro, T.-H. Yong, P. E. Laibinis, *Langmuir* **14** (1998) 6130
12. Z. L. Quan, S. H. Chen, Y. Li, X. G. Cui, *Corros. Sci.* **44** (2002) 703
13. H. Y. Ma, S. H. Chen, L. Niu, S. X. Shang, S. L. Li, S. Y. Zhao, Z. L. Quan, *J. Electrochem. Soc.* **148** (2001) B208
14. H. Y. Ma, S. H. Chen, B. S. Yin, S. Y. Zhao, X. Q. Liu, *Corros. Sci.* **45** (2003) 867
15. C. T. Wang, S. H. Chen, H. Y. Ma, C. S. Qi, *J. Appl. Electrochem.* **33** (2003) 179
16. A. T. Lusk, G. K. Jennings, *Langmuir* **17** (2001) 7830
17. Y. Feng, W. K. Teo, K. S. Siow, Z. Gao, K. L. Tan, A. K. Hsieh, *J. Electrochem. Soc.* **144** (1997) 55
18. Z. Quan, X. Wu, S. Chen, S. Zhao, H. Ma, *Corrosion* **57** (2001) 195
19. H. P. Lee, K. Nobe, *J. Electrochem. Soc.* **133** (1986) 2035
20. Y. Feng, K. S. Siow, W. K. Teo, A. K. Hsieh, *Corrosion* **53** (1997) 389
21. O. E. Barcia, O. R. Mattos, N. Pebere, B. Tribollet, *J. Electrochem. Soc.* **140** (1993) 2825
22. M. Braun, K. Nobe, *J. Electrochem. Soc.* **126** (1979) 1666
23. U. Bertocci, D. R. Turner, *Encyclopedia of the Electrochemistry of the Elements*, Vol. II, A. J. Bard, Ed., Marcel Dekker Inc., New York, 1974, p. 383
24. G. Brunoro, A. Frignani, A. Colledan, C. Chiavari, *Corros. Sci.* **45** (2003) 2219
25. S. Li, S. Chen, S. Lei, H. Ma, R. Yu, D. Liu, *Corros. Sci.* **41** (1999) 1273
26. X. Wu, H. Ma, S. Chen, Z. Xu, A. Sui, *J. Electrochem. Soc.* **146** (1999) 1847
27. A. V. Benedetti, P. T. A. Sumodjo, K. Nobe, P. L. Cabot, W. G. Proud, *Electrochim. Acta* **40** (1995) 2657
28. L. Sun, R. M. Crook, *Langmuir* **9** (1993) 1951
29. X.-M. Zhao, J. L. Wilbur, G. M. Whitesides, *Langmuir* **12** (1996) 3257
30. F. P. Zamborini, R. M. Crooks, *Langmuir* **14** (1998) 3279
31. E. Sabatani, J. Cohen-Boulakia, M. Bruening, I. Rubinstein, *Langmuir* **9** (1993) 2974
32. H. Fijumoto, S. Kato, S. Yamabe, K. Fukui, *J. Chem. Phys.* **60** (1974) 572
33. J. Vosta, J. Eliasek, P. Knizek, *Corrosion* **32** (1976) 183
34. J. Vosta, N. Hackerman, *Corros. Sci.* **30** (1990) 949
35. H. Ma, S. Chen, L. Niu, S. Zhao, S. Li, D. Li, *J. Appl. Electrochem.* **32** (2002) 65.